NONLINEAR OPTICAL PROPERTIES OF POTENTIAL SENSITIVE STYRYL DYES

JUNG YAW HUANG, AARON LEWIS, AND LESLIE LOEW*
*Department of Applied Physics, Cornell University, Ithaca, New York 14853; and *Department of Physiology, University of Connecticut Health Center, School of Medicine, Farmington, Connecticut 06032*

ABSTRACT The nonlinear optical properties of dyes that alter their optical characteristics rapidly with membrane potential are described. The second harmonic signals from these dyes characterized in this paper are among the largest that have been detected to date. Structural conclusions are drawn from the second harmonic signals generated by the Langmuir Blodgett monolayers used in these measurements. Our results indicate that with appropriate instrumentation second harmonic signals could readily be detected from living cells stained with these dyes.

INTRODUCTION

Recently, in cell biology, there has been great progress in synthesizing molecules that have rapid alterations in optical properties in response to electrical fields across cell membranes (1–5). In one class of molecules, the essential aspect that allows them to respond rapidly to such membrane potential variations appears to be a large alteration in the charge distribution within the chromophore in response to optical excitation (6). Thus, the effect of an electrical field is to perturb this light-induced charge distribution which causes a rapid and readily detectable effect on the absorption spectrum of the dye in question. In this paper the nonlinear optical properties of these dyes are studied, and it is demonstrated that they exhibit some of the largest second order nonlinear hyperpolarizabilities that have been measured thus far.

The dyes considered in this investigation were designed by the use of molecular orbital calculations that allowed the prediction of the molecular structures that would give the largest light-induced dipole alterations (7). As a result of these calculations molecules were synthesized that had negative charges that were covalently linked to a positively charged pyridinium styryl structure (8). The molecules chosen for this study are shown in Fig. 1.

To study the nonlinear optical properties of such molecules, we generated monolayer films of the pyridinium styryl dyes on a Langmuir trough (9). The structures of the films were investigated by observing their nonlinear optical properties (10, 11). The results of this study are consistent with the notion that these molecules have unique electro-optical characteristics.

Address reprint requests to Aaron Lewis, Division of Applied Physics, Bergmann Bldg., The Hebrew University of Jerusalem, Jerusalem, Israel.

EXPERIMENTAL PROCEDURES

A Q-switched frequency doubled Nd:YAG laser with a 10-Hz repetition rate and 10-ns pulsewidth was used. The Nd:YAG laser was adjusted to give a green 532-nm beam of <20 mW, which was focused onto a 3-mm diameter spot on the sample surface after passing through a half-wave plate, a Glan-Thompson laser prism polarizer, and a KG-5 color glass filter. The reflected second harmonic signal at a wavelength of 266 nm was passed through a UG-5 color glass filter which blocked the fundamental at 532 nm. The UG-5 filter was followed by a UV Glan-Taylor polarizer and a Schoeffel 0.2-m double monochromator. The SH signal was detected by a cooled RCA C31034 photomultiplier and averaged by a Stanford Research Model SR250 boxcar integrator.

The dyes were all synthesized by the aldol condensation or Pd-catalyzed coupling procedures as detailed by Hassner et al. (12). The spreading solutions were prepared by adding a specific amount of dye molecules into spectrophotometry grade chloroform (Fisher Scientific Co., Pittsburgh, PA) according to the published extinction coefficients (8). The molecules were spread on the surface of deionized distilled pure water subphase at pH 6.4.

The Langmuir trough was made out of Teflon. A movable barrier controlled the surface density of molecules and a #40 filter paper with dimension 0.7 × 1.0 cm was attached to a UC-3 force transducer (Gould Inc., Santa Clara, CA) to measure the surface pressure (13). During detection of the second harmonic signal, the movable barrier was controlled by a stepping motor such that the surface pressure of the film was kept at constant value.

Molecular orientation was determined by using the Heinz nulling technique (14). The incident pump beam was arranged to satisfy the following condition:

$$[\mathbf{e}_{\parallel}(\omega)/\mathbf{e}_{\perp}(\omega)]^2 = 2 \qquad (1)$$

where $\mathbf{e}(\omega)$ is the product of the polarization vector and the Fresnel factor for the pump field in the monolayer. The subscripts denote the components of $\mathbf{e}(\omega)$ on or perpendicular to the layer plane. This condition can be met by adjusting the pump beam to have an angle of incidence of 45° and a polarization of 35.3° away from the incident plane. The molecular orientation was determined by the second harmonic extinction direction, as indicated by the UV polarizer.

Our detection sensitivity was calibrated against the second harmonic intensity from an x-cut quartz plate, observed under the same experimental conditions. The quartz plate was rotated 28.75° about the *y*-axis of the

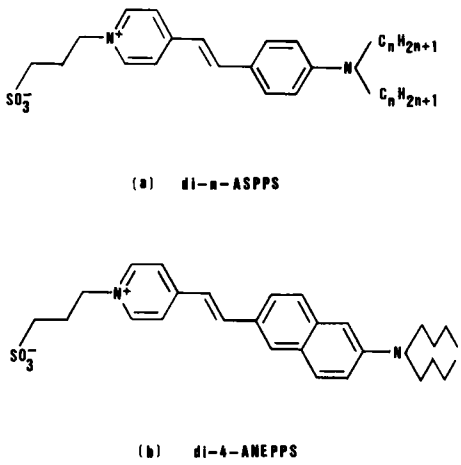

FIGURE 1 The chemical structures of (*a*) the di-*n*-ASPPS and (*b*) the di-4-ANEPPS dye molecules.

crystal to obtain one of the maxima of the Maker's fringes. The polarizations of the fundamental and second harmonic beams were chosen to be **p**-polarized relative to the plane of incidence. In this case, the two beams are the extraordinary waves of the quartz crystal. Using the known nonlinear second order susceptibility $d_{11} = 2.4 \times 10^{-9}$ esu (15) and the index of refraction (16) of quartz at 532 and 266 nm, we obtained a ratio of (17)

$$I_{p\to p}(2\omega)/[I_p(\omega)]^2 = 3.96 \times 10^{-26}\ \text{cm}^2\ \text{erg}^{-1}, \qquad (2)$$

where the first index in the subscript indicates the polarization of the fundamental beam and the second index for that of the second harmonic signal. The **p** (or **s**) denotes that the polarization vector is parallel (or perpendicular) to the plane of incidence. For measurements of dispersion of the dye molecular hyperpolarizabilities, a fundamental beam from a dye laser which was pumped by the Nd:YAG pulse laser was used. The same thin x-cut quartz plate was used as the calibration standard by assuming that the quartz plate has negligible dispersion for its second-order susceptibility.

RESULTS AND DISCUSSION

Monolayer Molecular Symmetry Properties

The **s**-polarized second harmonic (SH) intensity for the excitation of a **p**-polarized fundamental beam, $I_{p\to s}$, was measured to characterize the symmetry properties of the monolayer structure of the pyridinium styryl dyes that were the focus of this study. For the di-4-ANEPPS dye monolayer at 16 dynes/cm of surface presssure, the $I_{p\to s}$ is ~10% of the $I_{s\to p}$. The $I_{p\to s}$ SH intensity is proportional to the absolute square of the *xyz* component of the surface susceptibility tensor, $\chi^{(2)}_{xyz}$. This component vanishes if the Langmuir film possesses a mirror plane containing the trough surface normal. However, molecules without mirror planes cannot be arranged in such a way as to give the whole ensemble mirror symmetry. Thus when there is mirror symmetry, a mirror plane which contains the molecular long axis must exist in the molecule as well (18). The high value of $I_{p\to s}$ (10% of $I_{s\to p}$) that we observe indicates that although the chromophores have a mirror plane which contains the molecular long axis, the conformation in the monolayer may break this mirror symmetry.

Monolayer Molecular Orientation

There are two approaches to obtaining the angular orientation of the styryl dyes in the monolayer. The first method involves measuring and calculating the intensity of the SH signal under different polarization conditions, **s**, **p**, and 45°. A second method is to extinguish the SH signal by rotating a polarizer in the output beam relative to a fixed input polarization.

For the first approach, the SH intensities of $I_{s\to p}$ and $I_{p\to p}$ for di-4-ANEPPS and di-6-ASPPS monolayers at various surface pressures are compared in Fig. 2, *a* and *b*. In di-4-ANEPPS, the ratio of $I_{p\to p}/I_{s\to p}$ was found to decrease from 0.4 to 0.1 with the increase of the surface

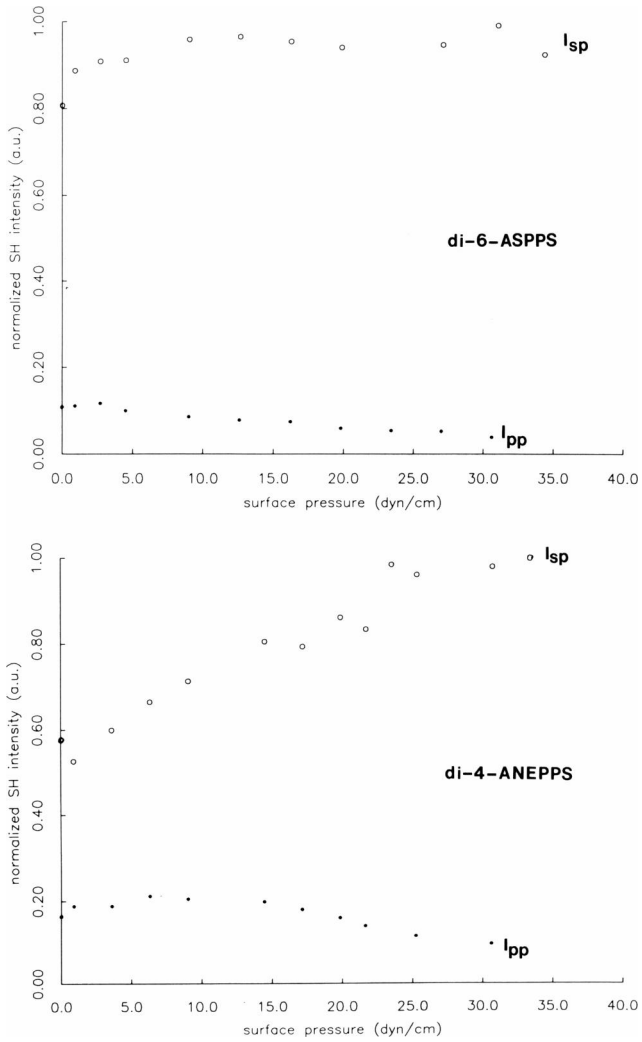

FIGURE 2 The second-harmonic (SH) intensities of styryl dye monolayers, (*a*) di-6-ASPPS and (*b*) di-4-ANEPPS, at different surface pressures. The **p**-polarized SH intensity with an **s**-polarized fundamental beam, $I_{s\to p}$, is shown in open circles. Solid circles are for $I_{p\to p}$ SH intensity generated by a **p**-polarized fundamental beam. The laser beam was set at an incident angle of 45° in all experiments.

pressure for the monolayer. For di-6-ASPPS monolayer, this ratio was found to decrease from 0.12 at 0 dynes/cm of surface pressure to 0.05 at high surface pressure. To understand the difference of this variation in the $I_{p\to p}$ to $I_{s\to p}$ ratio between the two monolayers, calculations were performed using previously derived equations (19), and the results are shown in Fig. 3 where the intensities of three different polarized SH beams, $I_{s\to p}$, $I_{p\to p}$, and $I_{45\to p}$, are plotted at various incident angles. To calculate these intensities as a function of the incident laser angle, three quantities are needed. These quantities are the components of the hyperpolarizability tensor, β, the orientational parameter, ψ, which is the angle between the molecular plane and the water surface and the molecular inclination angle, θ, which is the polar angle of the molecule relative to the normal surface. The two in-plane components of the molecular hyperpolarizability tensor, β_{ZZZ} and β_{ZXX}, are dominant for these types of molecules as reported by Dirk et al. (20). The values estimated by Dirk et al. are $\beta_{ZZZ} = 6 \times 10^{-28}$ esu and $\beta_{ZXX} = -3.6 \times 10^{-28}$ esu. For the calculation, the orientational parameter, ψ, was assumed to be either randomly distributed or equal to 0°. For the random distribution assumption the result for $I_{s\to p}$ is shown as a solid line in Fig. 3 and the $\psi = 0°$ assumption is shown as a curve with boxes. In the above calculations the molecular inclination angle, θ, was chosen to be 55° with a width of ±10°. The ratio of $I_{p\to p}/I_{s\to p}$ for the case of $\psi = 0°$ is found to be 0.47 at the incident angle of 45° but it becomes 0.08 for the case of ψ being randomly distributed.

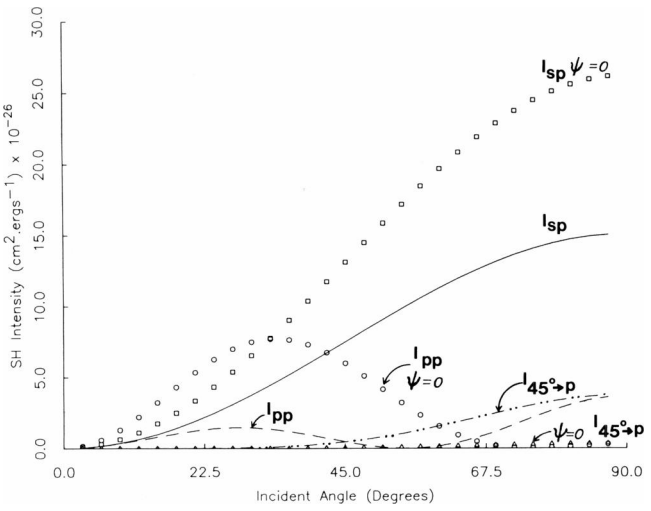

FIGURE 3 The calculated intensities of three different polarized second-harmonic beams, $I_{s\to p}$, $I_{p\to p}$, and $I_{45\to p}$, are plotted at various incident angles. The two most significant in-plane components of the model molecular hyperpolarizability tensor were chosen to be $\beta_{zzz} = 6 \times 10^{-28}$ esu and $\beta_{zxx} = -3.6 \times 10^{-28}$ esu, respectively. The molecular inclination angle, θ, has a central value of 55° with a width of ±10°. The orientational parameter, ψ, which is related to the angle between the molecular plane and the water surface, was assumed to be either randomly distributed (*solid line, dashed line, and dashed-dotted line*) or equal to 0° (shown in the curves with *open boxes, open circles,* and *open triangles*).

The measured value of $I_{p\to p}/I_{s\to p} = 0.4$ for di-4-ANEPPS monolayer with an incident angle of 45° and under low surface pressure indicates that the di-4-ANEPPS dye molecule due to its larger π-electron system and planar ring structure tends to contact the water surface with a preferred geometry of $\psi = 0°$. For the di-6-ASPPS monolayer, the geometry with the randomly distributed ψ angle is chosen since the measured ratio of $I_{p\to p}$ to $I_{s\to p}$ is found to be close to the values graphically represented in Fig. 3 for random systems. In Fig. 2, *a* and *b*, the small but finite value of $I_{p\to p}$ at an incident angle of 45° for the di-6-ASPPS and di-4-ANEPPS monolayers at all surface pressures indicates that the out-of-plane transition moment

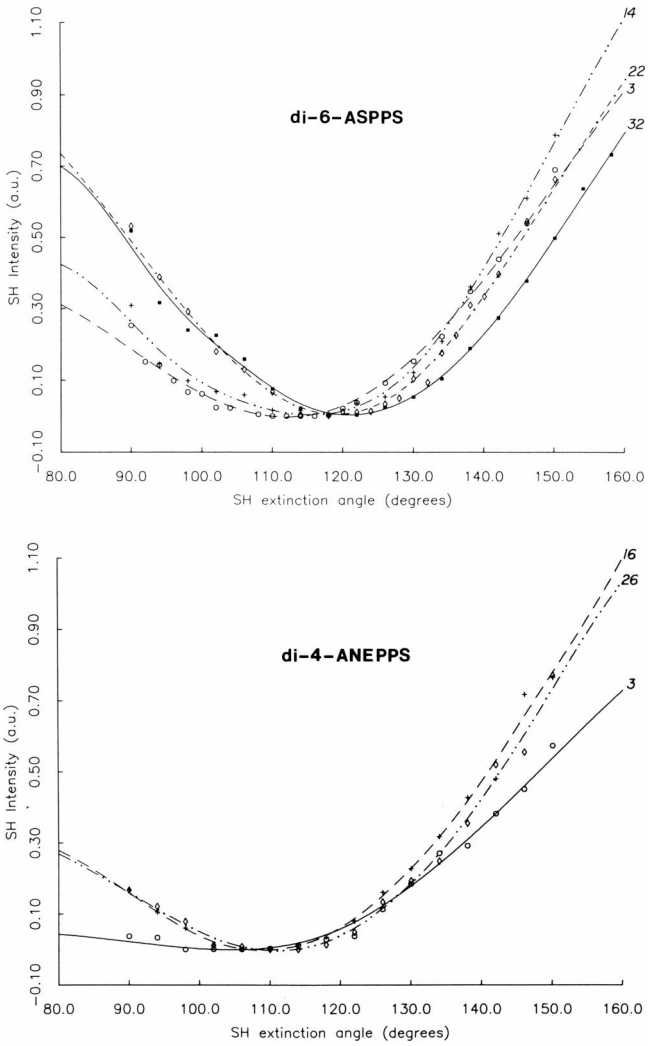

FIGURE 4 The extinction angle measurements of the second-harmonic (SH) beams for the (*a*) di-6-ASPPS monolayer at surface pressures of 3, 14, 22, and 32 dynes/cm and (*b*) di-4-ANEPPS monolayer at surface pressures of 3, 16, and 26 dynes/cm, respectively. The *x*-axis indicates the rotational angle of the SH beam polarization analyzer, where 90° corresponds to the **p**-polarized direction. The polarization of the incident pump beam is adjusted to be 35.5° from the plane of incidence. The lines in this figure are generated by a cubic spline fit to the experimental data (*symbols*) to guide the reader.

is small and that there is no single dominant component of the hyperpolarizability tensor.

As noted above an alternate approach to measure the molecular inclination angle, θ, in the monolayer is to measure the SH extinction angle. In Fig. 4 *a*, the extinction curves for di-6-ASPPS monolayer at surface pressures of 3, 14, 22, and 32 dynes/cm are shown. The angle of the polarization at which the minimum SH intensity was observed gradually increases with the surface pressure. The typical angle for this monolayer is ~120° when the surface pressure is ~22 dynes/cm. The same measurements were also made for the di-4-ANEPPS monolayer. Three extinction curves at surface pressures of 3, 16, and 26 dynes/cm are shown in Fig. 4 *b*. An extinction angle of 110° was observed for the monolayer when the surface pressure is above 16 dynes/cm. By choosing the molecular hyperpolarizability component $\beta_{zzz} = 9 \times 10^{-28}$ esu and a randomly distributed orientational parameter, ψ, three calculated SH extinction curves are shown in Fig. 5 for the molecular inclination angle θ = 50° (*solid line*), 55° (*dashed line*), and 60° (*dashed-dotted line*). The measured SH extinction data of di-6-ASPPS monolayer at a surface pressure of 3 dynes/cm (see Fig. 4 *a*) compares very well with the calculated curve for the molecular inclination angle of 55°. To fit satisfactorily the measured curves at surface pressures of 14, 22 and 32 dynes/cm, the molecular inclination angle had to be decreased to 51, 49, and 47°. Similar calculations were also made for the monolayer of the di-4-ANEPPS molecule with the molecular hyperpolarizability $\beta_{zzz} = 6 \times 10^{-28}$ esu and a randomly distributed orientational parameter ψ. Three curves with the molecular inclination angles of 55, 65, and 75° are shown in Fig. 5 *b*. Compared with the measured SH extinction data for the di-4-ANEPPS monolayer, the calculated curve with the inclination angle of 55° simulates quite well the measured SH extinction data at the surface pressures of 16 and 26 dynes/cm. The correlations of the measured and calculated SH extinction curves have revealed a reasonable picture that at low surface pressures the di-4-ANEPPS molecule with the more extended π-electron system tends to lie flatter on the water surface than the di-6-ASPPS molecule does. However, at high surface pressures both molecules exhibit approximately similar inclination angles.

The preceding discussion of the extinction angle and monolayer structure did not consider the observation of more than one contributing hyperpolarizability component. When molecules such as styryl dyes are considered, where there is not one dominant hyperpolarizability component (20), the effect of other components has to be considered especially when there are nonrandom distribu-

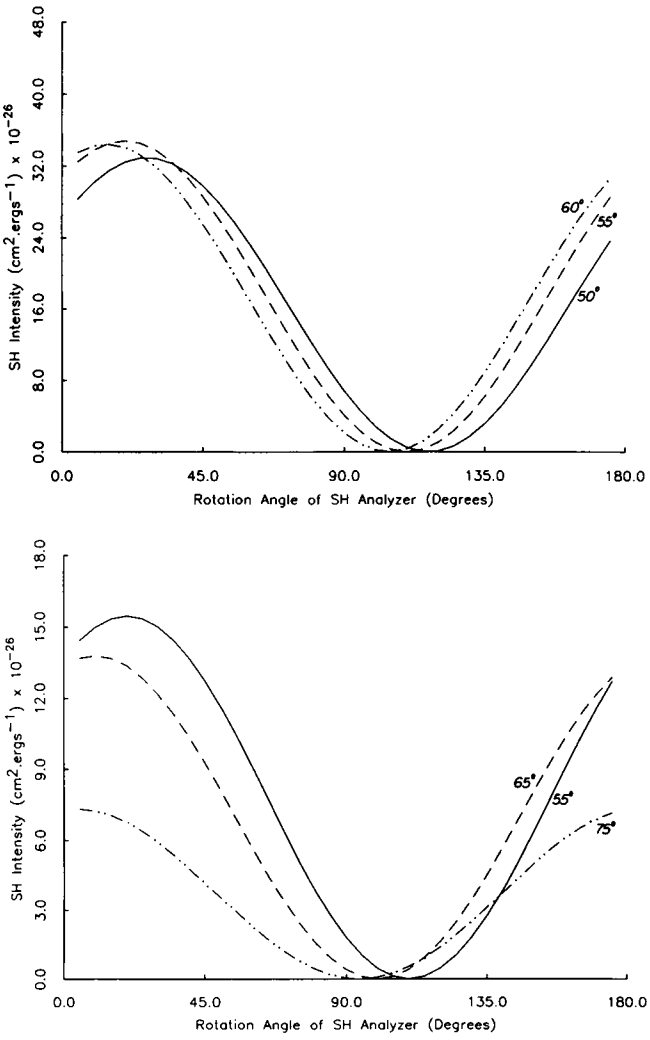

FIGURE 5 The calculated extinction curves of the SH beams from (*a*) di-6-ASPPS and (*b*) di-4-ANEPPS monolayers. The geometries of the pump and SH beams are the same as those described in Fig. 4. In this calculation, the orientational parameter, ψ, was assumed to be randomly distributed. The molecular inclination angle, θ, is indicated near the curves.

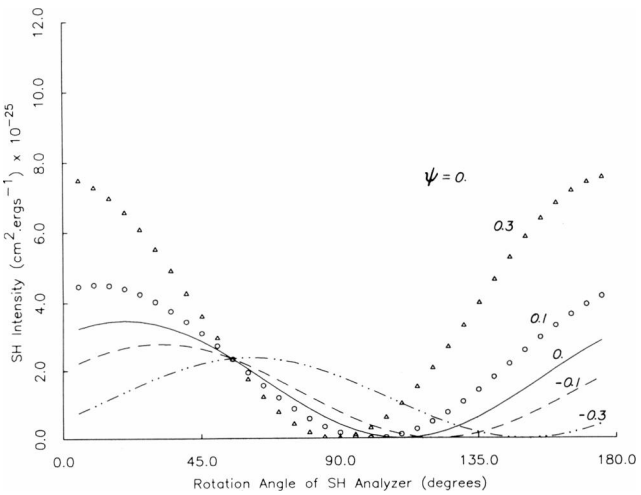

FIGURE 6 The calculated extinction curves of the SH beams under different values of β_{zxx}. In this calculation, the chosen parameters are θ = 55°, ψ = 0°, and $\beta_{zzz} = 6 \times 10^{-28}$ esu. The second hyperpolarizability component, β_{zxx}, was determined by a parameter r with the definition $r = \beta_{zxx}/\beta_{zzz}$ and this parameter was varied from −0.3 to +0.3.

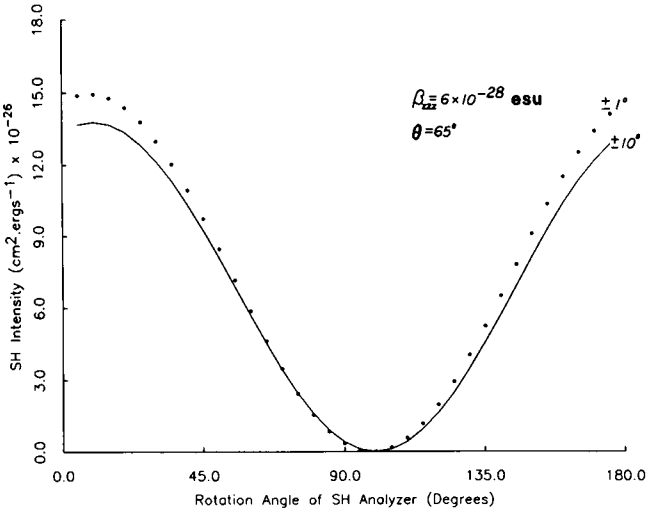

FIGURE 7 The same calculation as Fig. 5 *b* except that the molecular inclination angle, θ, was assumed to be 65° and with a spread of ±10° (*solid line*) and ±1° (*solid circles*), respectively.

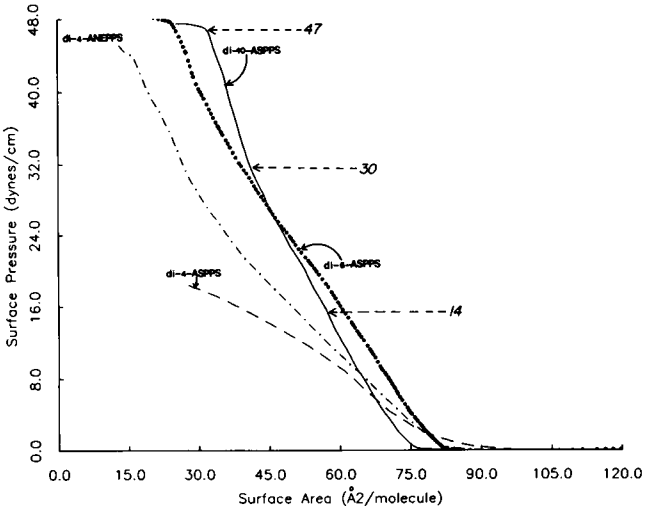

FIGURE 8 The surface pressure–surface area (π-A) isotherms of the di-4-ASPPS (*dashed line*), di-4-ANEPPS (*dashed-dotted line*), di-6-ASPPS (*solid circles*), and the di-10-ASPPS (*solid line*) for Langmuir–Blodgett monolayers on a 0.5 mM $CdCl_2$ water subphase (pH = 7), respectively.

tions of the molecular plane relative to the surface. Such conditions are exemplified by $\psi = 0°$. The results of calculating the extinction curves under the condition of $\psi = 0°$ where the effect of the β_{zxx} component has to be considered is shown in Fig. 6 for a defined inclination angle $\theta = 55° \pm 10°$. In this figure, the second hyperpolarizability component β_{zxx} was determined by a parameter r with the definition $r = \beta_{zxx}/\beta_{zzz}$ and this parameter was varied from -0.3 to $+0.3$. The direction of the SH polarization vector at which the minimum SH intensity is detected decreases from 152 to 90° as a function of r. The results in Fig. 6 indicate that for di-4-ANEPPS at low surface pressure where $\psi = 0°$ the inclination angle, θ, would be underestimated if β_{zxx} is not taken into account.

Our results yield little information on the width of the molecular inclination angle, θ. This is seen in Fig. 7 where two curves with widths of ±10 and ±1° are compared in a model calculation. No significant shifting and broadening of the SH extinction curve is observed indicating the lack of sensitivity of these measurements to the variation in inclination angle.

Wavelength Dependence

Dispersions for these dye molecular hyperpolarizabilities are listed in Table I. The SH measurements were performed at surface pressures of 14, 24, 24, and 17 dynes/cm for the di-4-ASPPS, di-6-ASPPS, di-10-ASPPS, and di-4-ANEPPS monolayers, respectively. At these surface pressures, the monolayers have a surface density of 2×10^{14} cm^{-2} (see Fig. 8 for the π-A isotherms). Resonance is observed as the SH photon energy approaches the absorption band of the dye molecules which were found to be ~480 nm for dye monolayers on glass substrates. For these molecules, the contribution from the water surface to the surface susceptibility could be neglected (9). Due to the lack of a near infrared laser,

TABLE I
DISPERSIONS OF THE SURFACE SUSCEPTIBILITIES OF THE PYRIDINIUM STYRYL DYE MONOLAYERS AT SURFACE DENSITY OF $N_S = 2 \times 10^{14}$ MOLECULES/cm^2

Wavelength	Di-4-ASPPS ($N_S = 2 \times 10^{14}$) $\chi^2_{zxx} \times 10^{-14}$	Di-6-ASPPS ($N_S = 2 \times 10^{14}$) $\chi^2_{zxx} \times 10^{-14}$	Di-10-ASPPS ($N_S = 2 \times 10^{14}$) $\chi^2_{zxx} \times 10^{-14}$	Di-4-ANEPPS ($N_S = 2 \times 10^{14}$) $\chi^2_{zxx} \times 10^{-14}$
nm				
532	1.2	1.2	1.2	0.8
546	0.4	0.4	0.4	0.4
560	0.4	0.4	0.4	0.5
584	0.7	0.7	0.7	0.8
604	1.0	1.0	0.9	1.0
624	0.8	0.8		0.8
640	1.3	1.3	1.3	1.4
660	2.5	2.4	2.4	2.5
1064	1.7	1.7	1.9	2.1

dispersions above 680 nm were not measured except for the measurement at 1.06 μm generated by the fundamental beam of the Nd:YAG laser. The replacement of the phenyl ring of di-*n*-ASPPS molecules by the naphthalene of di-4-ANEPPS has little effect on the SHG properties of these dye molecules.

CONCLUSION

The second-order nonlinear optical responses of four types of pyridinium styryl dye molecules with different lengths of π-electron systems and hydrocarbon side chains were measured in this study. The correlations of the measured and calculated SH extinction curves have revealed that the di-4-ANEPPS molecule tends to lie flatter on the water surface than the di-6-ASPPS molecule. The experiments also indicate that the tilt angle between the plane of the di-4-ANEPPS molecule and the water surface is not randomly distributed at low surface pressure and this allows for interactions between the water surface and the nonpyridinium nitrogen of the dye that cannot take place at high surface pressure.

Based on these second harmonic measurements we are now in a position to estimate whether such signals could be detected in live cells stained with such dyes. For the measurement of cell membrane potential with these dyes using fluorescence detection, a concentration of ~1% relative to membrane lipid is typically attained. This would yield a surface susceptibility of 2×10^{-16} esu for di-4-ANEPPS at 1.06 μm and such a signal can be detected even in our low repetition rate system. If a mode-locked Nd:YAG laser system with a 10 ps pulsewidth and 10 MHz repetition rate is used, the signal intensity could increase by several orders (21). The infrared nature of the light source should be specifically important in preventing damage mechanisms induced by the laser and thus allowing for extended illumination without bleaching. In addition, the molecules endocytotically internalized into the cell will not contribute to the observed signal. Therefore, simply those molecules in the membrane that are responding to the membrane potential will be responsible for the signal without any background from internalized dye molecules. Thus, for all of these reasons the study of alterations in the surface susceptibility as a function of changes in cell membrane potential should be most interesting. Furthermore, because the second harmonic signal is generated instantaneously the only limitation to the kinetic detection of membrane potential with this technique is the response time of the dye. For the dyes we have investigated, this response time is thought to be nanoseconds or better.

This research was supported by a grant from the United States Air Force Grant #AFOSR-87-0381 to A.L. L.M. is pleased to acknowledge support from the United States Public Health through National Institutes of Health Grant GM 35063.

Received for publication 18 August 1987 and in final form 3 December 1987.

REFERENCES

1. Grinvald, A. 1985. Real-time optical mapping of neuronal activity: from single growth cones to the intact mammalian brain. *Annu. Rev. Neurosci.* 8:263–305.
2. Loew, L. M. 1988. How to choose a potentiometric membrane probe. *In* Spectroscopic Membrane Probes. L. M. Loew, editor. CRC Press, Inc., Boca Raton, FL. Ch. 14.
3. London, J. A., D. Zecevic, L. M. Loew, H. S. Ohrbach, and L. B. Cohen. 1986. Optical measurement of membrane potential in simple and complex nervous systems. *In* Fluorescence in the Biological Sciences. D. L. Taylor, A. S. Waggoner, F. Lanni, R. F. Murphy, and R. Birge, editors. Alan R. Liss, Inc., New York. 423–447.
4. Salzberg, B. M. 1983. Optical recording of electrical activity in neurons using molecular probes. *In* Current Methods in Cellular Neurobiology. J. L. Barker and J. F. McKelvy, editors. John Wiley and Sons, New York. 139–187.
5. Waggoner, A. S. 1985. Dye probes of cell, organelle, and vesicle membrane potentials. *In* The Enzymes of Biological Membranes. A. N. Martonosi, editor. Plenum Publishing Corp., New York. 313–331.
6. Loew, L. M. 1982. Design and characterization of electrochromic membrane probes. *J. Biochem. Biophys. Methods.* 6:243–260.
7. Loew, L. M., G. W. Bonneville, and J. Surow. 1978. Charge shift probes of membrane potential. Theory. *Biochemistry.* 17:4065–4071.
8. Fluhler, E., V. G. Burnham, and L. M. Loew. 1985. Spectra, membrane binding and potentiometric responses of new charge shift probes. *Biochemistry.* 24:5749–5755.
9. Rasing, Th., G. Berkovic, Y. R. Shen, S. G. Grubb, and M. W. Kim. 1986. A novel method for measurements of second-harmonic nonlinearities of organic molecules. *Chem. Phys. Lett.* 130:1–5.
10. Rasing, Th., Y. R. Shen, M. W. Kim, P. Valint, Jr., and J. Bock. 1985. Orientation of surfactant molecules at a liquid-air interface measured by optical second-harmonic generation. *Phys. Rev. Lett.* 31:537–539.
11. Shen, Y. R. 1986. Surface second harmonic generation: a new technique for surface studies. *Annu. Rev. Material Sci.* 16:69–86.
12. Hassner, A., D. Birnbaum, and L. M. Loew. 1984. Charge shift probes of membrane potential. Synthesis. *J. Org. Chem.* 49:2546–2551.
13. Gaines, G. L., Jr. 1965. Insoluble Monolayer at Liquid-Gas Interfaces. John Wiley and Sons, New York. 30–128.
14. Heinz, T. F., H. W. K. Tom, and Y. R. Shen. 1983. Determination of molecular orientation of monolayer adsorbates by optical second-harmonic generation. *Physical Rev.* 28:1883–1885.
15. Shen, Y. R. 1984. The Principles of Nonlinear Optics. John Wiley and Sons, New York. 101.
16. Philipp, H. R. 1985. Handbook of Optical Constants of Solids. E. D. Palik, editor. Academic Press, New York. 719–747.
17. Jerphagnon, J., and S. K. Kurtz. 1970. Maker fringes: a detailed comparison of theory and experiment for isotropic and uniaxial crystal. *J. Appl. Physics.* 41:1667–1681.
18. Dick, B. 1985. Irreducible tensor analysis of sum- and difference-frequency generation in partially oriented samples. *Chem. Phys.* 96:199–215.
19. Mazely, T. L., and W. M. Hetherington III. 1987. Second-order susceptibility tensors of partially ordered molecules on surfaces. *J. Chem. Phys.* 86:3640–3647.
20. Dirk, C. W., R. J. Twieg, and G. Wagniére. 1986. The contribution of π electrons to second harmonic generation in organic molecules. *J. Am. Chem. Soc.* 108:5387–5395.
21. Boyd, S. T., Y. R. Shen, and T. W. Hänsch. 1986. Continuous-wave second-harmonic generation as a surface microprobe. *Opt. Lett.* 11:97–99.